UJMR, Vol. 8 No. 2, December, 2023, pp. 74 - 85 *E-ISSN: 2814 – 1822; P-ISSN: 2616 – 0668*

https://doi.org/10.47430/ujmr.2382.009

Received: 16 October 2023 **Accepted:** 27 November 2023

Synthesis of Zinc Oxide Nanoparticles using Extract of *Cynodon dactylon* and Assessment of their Biological Activity against *Staphylococcus aureus* and *Escherichia coli*

[*1]Anuforo, H. U., [2]Ogbulie, T. E., [2]Udebuani, A. C. and Ezeji, E. U.

[1]Department of Biology, School of Biological Sciences, Federal University of Technology, PMB 1526, Owerri, Nigeria.

[2]Department of Biotechnology, School of Biological Sciences, Federal University of Technology, PMB 1526, Owerri, Nigeria.

***Corresponding Author:** henry.anuforo@futo.edu.ng; +234-8066583404

Abstract

Nanotechnology is a groundbreaking technology that that has been widely applied in creating materials which are useful in various fields. It's important to maintain eco-friendly approaches for synthesis of nanoparticles by diversifying the substrate sources. In this study, the researchers used aqueous extract of Cynodon dactylon to synthesize zinc oxide nanoparticles (ZnONPs). Quantitative phytochemical analysis of the extract showed high concentrations of alkaloids, flavonoids, carbohydrates, proteins, amino acids, and phenolic compounds. In contrast, moderate concentrations of tannins, oils, and fats, and low concentrations of phlorotannins, saponin, triterpenoids, and cardiac glycosides were found. Sterols, anthraquinone glycosides, gums, and mucilages were not detected in the extract. The synthesized ZnONPs showed absorbance ranging from 293 nm to 336 nm, with a peak at 307 nm. Fourier transform infrared (FTIR) spectroscopy revealed that the surface of the ZnONPs contained alcohol (intermolecular bonded), alkyne, amine salt, alkane, alkyne, aromatic compounds, conjugated alkene, amine, nitro compound, sulfonyl chloride, alkyl aryl ether, and sulfoxide. Dynamic light scatering (DLS) analysis of the ZnONPs showed that its average size was 35.34±1.64 nm, and the polydispersity index was 0.6335. Spectrum of X ray diffraction indicated that peaks formed at 2θ and their corresponding orientation planes are 31.92° (100), 34.62° (002), 36.44° (101), 47.64° (102), 56.84° (110), 63.3° (200), and 68.16° (112). Transmission electron micrograph revealed the spherical shape, and non-uniform sizes of ZnONPs, which ranged from 0.52 nm to 8.32 nm. Antibacterial analysis of biosynthesized ZnONPs recorded 16±3.2 mm and 6.0±2.2 mm; 6.7±2.1 mm and 4.33±1.3 mm, 0.0±0.0 mm and 1.0±1.41 mm, against Staphylococcus aureus and Escherichia coli, at 53.3 mg/mL, 26.7 mg/mL and 13.3 mg/ml concentrations, respectively. At sub-inhibitory concentrations, biosynthesized ZnONPs demonstrated effective dose-dependent antibiofilm formation activity against E. coli and S. aureus. Consequently, extract of Cynodon dactylon is suitable for biosynthesis of ZnONPs with effective antibacterial and antibiofilm formation activities.

***Keywords:** Cynodon dactylon, nanoparticles, antibacterial, biosynthesis, nanotechnology*

INTRODUCTION

Nanoparticles or nano-size particles refer to particles with at least one of their x, y, and z dimensions measured in the nanoscale range of 1 – 100 nm, or billionths of a meter (Turan *et al.*, 2019). These particles are outstanding scientific and technological breakthroughs that have proven useful in diverse areas of medicine, agriculture, electronics, pharmaceuticals and chemicals (Thakur *et al.*, 2022). Synthesis of nanoparticles with specific desired morphology, including size, shape, and crystalline structure, is critical to their successful applications as catalysts, antimicrobial agents, biomedical materials, biosensors and cheaper electrodes (Bukhari *et al.*, 2021). For instance, studies have shown that antibacterial efficacy of nanoparticles against *Micrococcus luteus* and *Escherichia coli* was affected by their shapes, with the highest activity found in spherical nanoparticles, followed by ellipsoidal and prismatic nanoparticles (Al-Shabib *et al.*, 2018, El-Hawary *et al.*, 2021).

Considering its green, cheaper and sustainable advantages, the biological synthesis method has dominated current studies, compared to chemical and physical synthesis methods. Generally, "green synthesis" describes the creation of nanoparticles through processes that do not involve any toxic chemicals or adversely impact the environment (Gungure *et*

al., 2021). Consequently, many researchers have reported the biosynthesis of various types of nanoparticles using extracts of different plants, including vanadium oxide nanoparticles (V_2O_5NPs) using *Punica granatum* (Angham and Lekaa, 2023), zinc oxide nanoparticles (ZnONPs) using hydroethanolic extract of *Leonotis nepetaefolia* leaves (Dubey *et al.*, 2023), biosynthesis of ZnONPs using plant extracts (El-Hawary *et al.*, 2021), ZnONPs using orange fruit peel extract (Thi *et al.*, 2020), silver nanoparticles (AgNPs) using *Mangifera indica* and *Prunus dulcis* extracts (Akujobi *et al.*, 2020), and AgNPs using *Borago officinalis* leaves extract (Kumavat and Mishra, 2021). Most of these plants are either medicinally or economically important. It is our informed opinion that continuous dependence on these plant sources for medicinal, economic and additionally, biosynthesis of nanoparticles, could trigger their over-exploitation. Hence, there is need to diversify the sources of plant extracts used in synthesis of nanoparticles, away from these medicinal and economically important plants.

A mechanism for the biosynthesis of ZnO using plant extracts has been suggested by Thi *et al.* (2020), which involves the ligation of the zinc precursor and the functional groups of plant extract, such as flavonoid, carotenoids, limonoid etc. These plant extract components contain hydroxyl aromatic ring, which forms complex ligands with zinc ions. Then nanoparticles are stabilized and formed during nucleation, and shaping. The resulting combination of plant extract components and zinc ions decomposes on calcination at 400 °C, releasing ZnO nanoparticles (Figure 1).

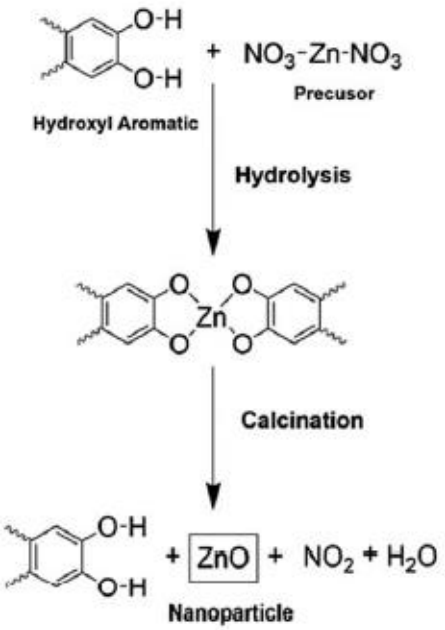

Figure 1: The chemical mechanism of ZnO nanoparticle formation. Adopted from Thi *et al.* (2020)

In view of increasing reduction in the efficacies of organic antibacterial agents due to their susceptibility to processing conditions, such as pressure, and high temperature, alternative use of inorganic antibacterial agents has become attractive to many researchers (Thi *et al.*, 2020). These inorganic materials, especially metal oxides, exert strong antibacterial activity even at low concentrations. They are also more stable at high pressures, and temperatures, with added longer shelf-life than their organic counterparts (Taylor *et al.*, 2013). Studies have revealed that metal oxide nanoparticles and metallic nanoparticles have become the most widely used inorganic antibacterial materials (Thi *et al.*, 2020), with promising improvement in microbial control. Also, metal nanoparticles have proven very useful in controlling the spread of diseases, in medical facilities, and to effectively fight against rampaging multidrug-resistant pathogens. Zhao *et al.*, (2023) reported that metal nanomaterials' high mobility, efficiency, and stability have presented them as an alternative disinfection technology. The mechanisms of antimicrobial activities of metal materials have been categorised into three, including the liberated metal ions effect, contact-killing effect, and reactive oxygen species (ROS) effect (Zhao *et al.*, 2023).

Specifically, zinc oxide is a well-known semiconducting inorganic material that can exist in three different crystal structures, including wurtzite, rock salt and zinc blende. Its wurtzite structure is thermodynamically stable at room temperature, in which all the zinc atoms are tetrahedrally coordinated with four oxygen atoms (Kulkarni *et al.*, 2011). With

a wide band gap of 3.1–3.3 eV, ZnO has been applied as biosensors, drug carriers, cosmetics, and antibacterial agents (Thi *et al.*, 2020). Presently, the US Food and Drug Administration has approved its use as a drug delivery mechanism (Dubey *et al.*, 2023). It is also cheaper, less poisonous, and more biocompatible than many other metal oxide nanoparticles (Smaoui *et al.*, 2023). Studies have shown that bulk pharmaceutically active compounds do not interact with ZnONPs (Dubey *et al.*, 2023).

Thus, some pertinent research questions which would arise include, does *C. dactylon* extract contain phytochemicals that are capable of reducing and capping metal precursors to form nanoparticles? Also, will resulting ZnONPs possess biological activity against known bacterial isolates? Achievement of viable answers to these questions would immensely contribute to the sustainability and relevance of biological method of nanoparticles synthesis.

MATERIALS AND METHODS

Reagents used

In this study, zinc nitrate hexahydrate ($Zn(NO_3)_2 \cdot 6H_2O$) (Merck, India Ltd), distilled water (Chemisciences, Nigeria) Ciprofloxacin (Maxicare Medical Laboratory, Nigeria), Nutrient agar, Brain Heart Infusion Broth, and Mueller Hinton's agar (Titan Biotech, Rajastan, India) were procured from their suppliers in Nigeria. All reagents were used as supplied, without further purifications.

Collection and processing of plant samples into extract

Healthy leaf samples of *Cynodon dactylon* Pers. (Bermuda grass) used as a source of extract in this study were collected from the Federal University of Technology, Owerri, Nigeria campus. Upon validation at the Department of Biology, Federal University of Technology, Owerri, Nigeria, the leaf samples were sorted, thoroughly washed with clean water and dried to constant weight under the sun. Subsequently, dried leaf samples were ground into fine powders, using a clean pestle and mortar before storing them in stoppered containers. Following the method of Akujobi *et al.*, (2020), aqueous extract of *Cynodon dactylon* was prepared by adding 1500 mL of distilled water into 107 g of ground sample in a 2000 mL conical flask. After boiling for 20 minutes and cooling to room temperature, it was filtered through Whatman No. 1 filter paper, and the resulting filtrate was preserved, in the refrigerator, for biosynthesis of nanoparticles. Following the method of Mahamadi and Wunganayi (2018), filtrate concentration was measured. This was done by evaporating 10 mL of the filtrate in a known-weight crucible to dryness in a hot air oven. It was done in triplicates and their average weight per millilitre of water was computed.

Phytochemical analysis of *Cynodon dactylon* extract

Qualitative phytochemical analysis of aqueous extract of *Cynodon dactylon* was conducted to determine its phytochemical compositions.

i. Benedict's test for carbohydrates

Test for carbohydrates was carried out by measuring 1 mL of Benedict's reagent into 1 mL of plant filtrate. Then the mixture was heated for 2 minutes in a boiling water bath. The appearance of characteristic coloured precipitate confirmed the presence of carbohydrates (Raaman, 2006).

ii. Wagner's test for alkaloids

Test for alkaloids was done by carefully adding a few drops of Wagner's reagent to the side of a test tube containing some quantities of the plant extract. The appearance of reddish-brown precipitate confirmed positive test (Ejikeme *et al.*, 2014).

iii. Test for saponin

This test was done by pipetting 3 mL of distilled water into a test tube containing 0.3 g of ground plant sample. After boiling the mixture for 10 minutes in a water bath, it was filtered with Whatman No 1 filter paper. Then, 5 mL of distilled water was mixed with 1 mL of the filtrate and vigorously shaken. Formation of stable, persistent froth and emulsion with addition of three drops of olive oil confirmed a positive test (Ejikeme *et al.*, 2014).

iv. Ferric chloride test for tannins

The test was carried out by putting a few drops of 5% ferric chloride ($FeCl_3$) solution into 1 mL of the plant extract. The appearance of greenish-black colour confirmed positive test for catecholic tannins, blue colour confirmed gallic tannins; and greenish-brown colour confirmed presence of condensed tannins (Ejikeme *et al.*, 2014).

v. Test for phlorotannins

Test for phlobatannins was carried out by adding 3 mL of distilled water to 0.3 g of plant sample and boiling for 20 minutes of extraction. Then, 5 mL of 1% aqueous hydrochloric acid was added to 10 mL of the aqueous extract of the plant sample and boiled. The appearance of red precipitate confirmed the positive test (Ejikeme *et al.*, 2014).

vi. Test for sterols and triterpenoids

The presence of sterols and triterpenoids in the plant sample was screened by adding 3 mL of distilled water in 0.3 g of the plant sample and extracting for 2 hours. Then, a mixture of 3 mL concentrated tetraoxosulphate (VI) acid and 2 mL chloroform was added to 5 mL of the

extract to form a layer. The appearance of red coloured lower layer was a confirmation of a positive test for sterols, while yellow coloured layer confirmed the presence of triterpenoids (Ejikeme *et al.*, 2014).

vii. Millon's test for proteins and amino acids

The plant sample was tested for proteins and amino acids by adding 10 ml of distilled water into 5 g of plant sample. After extraction and filtering, a few drops of Millon's reagent were added to 2 mL of filtrate. The appearance of white precipitate confirmed positive test (Raaman, 2006).

viii. Alkaline reagent test for flavonoids

The presence of flavonoid was tested by adding a few drops of sodium hydroxide to a small quantity of the plant extract. The appearance of colourless solution confirmed a positive test on the addition of dilute acid (Saxena *et al.*, 2013).

ix. Lead acetate test for phenolic compounds

The phenolic compounds were tested by mixing 1 mL of the plant extract with a few drops of 10% lead acetate solution. The appearance of white precipitate confirmed a positive test (Ejikeme *et al.*, 2014).

x. Spot test for fixed oils and fats

Fats and fixed oil were tested by pressing a small quantity of extract between two filter papers. Observation of oil stains on the paper confirmed positive (Banu and Catherine, 2015).

xi. Keller-Killani test for cardiac glycoside

Test for cardiac glycoside was carried out by 2 mL of the extract with glacial acetic acid, concentrated sulphuric acid and then one drop of 5% ferric chloride. The reddish-brown colour at the interface of the two liquid layers confirmed a positive test (Ejikeme *et al.*, 2014).

xii. Borntrager's test for anthraquinone glycosides

The presence of anthraquinone glycosides was tested by adding dilute sulphuric acid to 3 mL of extract, followed by boiling and filtering. Then, equal volumes of chloroform and filtrate were mixed after cooling extract. The organic layer was gently decanted, and ammonia was added. The appearance of pink or red at the ammonical layer confirmed a positive test (Ejikeme *et al.*, 2014).

xiii. Test for gums and mucilages

Screening for gums and mucilages was done by adding 25 mL of absolute alcohol into 10 mL of aqueous extract and constantly stirring. Then, it is filtered. The appearance of swelling properties after drying precipitate in air, confirmed positive test (Ejikeme *et al.*, 2014).

Biosynthesis of zinc oxide nanoparticles

The biosynthesis of zinc oxide nanoparticles (ZnONPs) used in this study was carried out as described by Thi *et al.* (2020). Ten millilitres (10 mL) of prepared aqueous extract of *Cynodon dactylon* and 90 mL of 0.05 M zinc nitrate hexahydrate ($Zn(NO_3)_2 \bullet 6H_2O$) were separately measured into a 250 mL conical flask. Their temperature was adjusted to 80 °C by placing and stirring them in a water bath set at 80±2 °C. Then, the pH of the plant extract was increased to 10 by adding few drops of 0.1 M NaOH. The two solutions were then reacted with each other by mixing and continuously stirring them at 80 °C for 30 minutes. The reacting mixture was kept in the dark, at room temperature, for 24 h to allow biosynthesis to proceed. Colour changes during the biosynthesis were visually observed and recorded. The absorbance of the resulting ZnO nanoparticles suspension was determined at 390 nm, using ultraviolet – visible spectrophotometer (Thermo Scientific, BioMate 3S, USA). This was used to compute the concentration of biosynthesised ZnONPs in the suspension. Centrifugation of the suspension was done to sediment ZnO nanoparticles at 4000 rpm for 30 min. After decanting the supernatant, the remaining ZnONPs were washed three times by adding distilled water, centrifuging at 4000 rpm and decanting the supernatant in each case. Finally, washed ZnONPs was stored at room temperature for further characterization.

Characterization of as-prepared ZnONPs

Characterization of zinc oxide nanoparticles biosynthesized in this study, using aqueous extract of *Cynodon dactylon*, was done to ascertain their properties. Spectrophotometric method (Thermo Scientific, BioMate 3S, USA) was used to determine its UV-visible absorbance spectrum within 200 – 800 nm wavelengths, in 2 mL quartz cuvette of 1 cm path length (Dubey *et al.*, 2023). Fourier transform infrared (FITR) spectroscopy was used to determine the functional groups in the ZnONPs. This was done by uniformly dispersing the biosynthesized ZnONPs in matrices of dry KBr. After compressing it into transparent disc, KBr was used as a standard, and it was analysed by scanning the spectrum within 4000-650 cm^{-1} range, at a resolution of 8 cm^{-1}. Malvern Zen 3600 (Zitasizer) instrument was used to determine the size distribution of ZnONPs solution (Amini *et al.*, 2017). X-ray diffraction (X'pert Panalytical) was carried out to determine the crystalline composition, including composition, phase texture, crystal orientation or structure of biosynthesized

ZnONPs. It was operated at a current of 30 mA, and voltage of 40 kV, with Cu K (α) radiation (Erdogan *et al.*, 2019). Transmission electron microscope (TEM) (Jeol 200CX) was used to determine the morphology and size of the biosynthesized ZnONPs, and ImageJ software was used to analyse the resulting photomicrograph.

Assessment of antibacterial activity of ZnO nanoparticles from *Cynodon dactylon* extract

The antibacterial activities of ZnONPs biosynthesized using aqueous extract of *Cynodon dactylon* was assessed against clinical isolates of *Escherichia coli* and *Staphylococcus aureus*. Identified isolates were collected from the Laboratory Unit of the Federal Medical Centre, Owerri, Imo State. Each isolate was aseptically sub-cultured on nutrient agar, and its identity was validated by culturing on appropriate selective and differential media, and observing their colonial morphology Eosin Methylene Blue (EMB) was used for *E. coli*, while Mannitol Salt Agar (MSA) was used for *Staphylococcus aureus*.

Agar well diffusion described by Chauhan et al. (2020) was adopted to determine the antibacterial activity of ZnONPs, and was carried out in duplicates. In each case, a loopful of each bacterial pure culture was inoculated into 5 mL of nutrient broth, and incubated for 24 hours, at 37 ºC. Then standardization of inoculum was done by comparing its turbidity to that of 0.5 McFarland solution (~10^8 cfu/mL). This was followed by aseptically spreading 0.1 mL of each standardized test inoculum onto surface of Mueller-Hinton (MH) agar plates.

Furthermore, two-fold dilutions of the biosynthesized ZnONPs weres prepared to give 53.3 mg/mL, 26.7 mg/mL and 13.3 mg/mL concentrations. Sterilized borers were used to aseptically bore four 1 mm wells on each MH agar plate. Then 0.5 mL of each of the prepared concentrations of ZnONPs was dispensed into appropriately labelled wells. The plates were allowed for some minutes for the nanoparticles suspension to be absorbed by the media. Ciprofloxacin disc (30 mg) and sterile distilled water were used as positive and negative controls respectively. After incubating all the plates at 37 °C, for 24 hours, the zones of inhibition (ZoI) formed were measured and recorded in mm (Aritonang *et al.*, 2019).

Assessment of antibiofilm formation activity of ZnO nanoparticles from *Cynodon dactylon* extract

Assessment of antibiofilm formation properties of ZnONPs was carried out in duplicates, using sub-bactericidal concentrations, following the tube method described by Landage *et al.* (2020). In each replicate, solution of Brain Heart Infusion Broth (BHI) + sucrose (2%) was prepared. After sterilization and cooling, 15 mL of the broth was pipetted into each of 8 test tubes, grouped into two; each of which was used for inoculation of either *Staphylococcus aureus* or *Escherichia coli*. Different concentrations (53.3 mg/mL, 26.7 mg/mL and 13.3 mg/mL) of ZnONPs, biosynthesized using aqueous extract of *Cynodon dactylon*, were prepared. Then 0.5 mL of each concentration of ZnONPs was added into appropriately labelled test tubes, which resulted in final concentrations of 1.76 mg/mL, 0.88 mg/mL and 0.44 mg/mL. Then 0.5 mL each of *Staphylococcus aureus* and *Escherichia coli* broths was inoculated into their appropriately labelled test tubes, after adjusting their turbidity to 0.5 McFarland standard. Inoculated BHI + sucrose containing test tubes, without addition of ZnONPs were used as negative controls. Afterward, all test tubes were incubated at 37°C for 24 hours. Analysis of antibiofilm-formation potential of the nanoparticles was done by decanting the culture in the glass tubes. After mild washing with distilled water, they were allowed to dry, before staining with 0.1% crystal violet solution. Excess stain was removed and tubes were washed with distilled water. After drying tubes in an inverted position, observation was made. Biofilm formation was considered positive when visible films lined the tube's wall and bottom. Ring formation at the liquid interface was not indicative of biofilm formation.

Statistical analysis

Given the duplication of the analyses, mean and standard deviations of all data from the studies were computed using Microsoft Excel 2010 and Minitab 17 software.

RESULTS

Results showed that average concentration of the aqueous extract of *Cynodon dactylon* leaf sample was 7.33±1.89 mg/mL, whereas the average pH was 6.5±0.9. The colour was brown.

Phytochemical composition of *Cynodon dactylon* extract

Table 1 shows the phytochemical composition of *Cynodon dactylon* extract. The result shows high concentrations of alkaloids, flavonoids, carbohydrates, proteins and amino acids, and phenolic compounds in the extract of *Cynodon dactylon*. There were moderate concentrations of tannins, oils and fats, but only slight concentrations of phlobatannins, saponin, triterpenoids and cardiac glycosides in the extract. On the other hand, sterols,

anthraquinone glycosides, gums and mucilages were not present in the extract.

Table 1: Phytochemical constituents of aqueous leaf extract of *Cynodon dactylon*

PHYTOCHEMICAL	INFERENCE
Alkaloids	+++
Phenolic compounds	+++
Carbohydrate	+++
Phlorotannins	+
Saponin	+
Sterols	-
Gums and mucilage	-
Proteins and amino acids	+++
Flavonoids	+++
Oil and fats	++
Triterpenoids	+
Anthraquinone glycosides	-
Tannins (catecholic tannins)	++
Cardiac glycoside	+

+++ implies high concentration; ++ implies moderate concentration; + implies slight concentration; and – means absent.

Concentration and size of zinc oxide nanoparticles biosynthesized with *C. Dactylon* extract

It was observed that during biosynthesis of ZnONPs, the colour of the extract changed from brown solution into dark-brown precipitate, on addition of the precursor solution. Results indicated that average concentration of resulting ZnONPs was 2.53±0.1 mg/mL, with average size of 36.99±0.7 nm.

Properties of ZnO nanoparticles biosynthesized using extract of *Cynodon dactylon*

Figure 2 show the absorbance spectrum of ZnONPs biosynthesized using extract of *Cynodon dactylon*. The spectrum revealed that the nanoparticle's absorbance range was from 293 nm to 336 nm, with a peak at 307 nm.

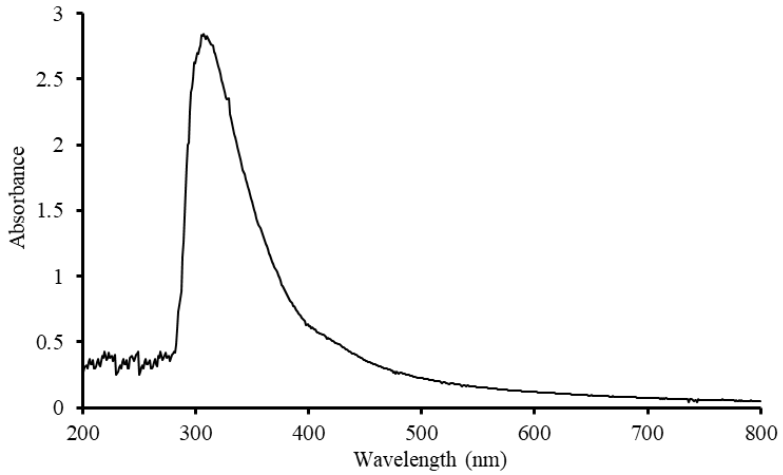

Figure 2: Absorbance spectrum for ZnONPs biosynthesized using aqueous extract of *Cynodon dactylon*.

Figure 3 is the spectrum obtained from FTIR anlysis of ZnONPs, biosynthesized with *Cynodon dactylon* extract. Many peaks were formed on the spectrum. Guided by prescriptions of Sigma-Aldrich (2023), the appeances of peaks, functional groups and compounds present were determined were identified, as presented in Table 2. Thus, alcohol (intermolecular bonded), alkyne, amine salt, alkane, alkyne, aromatic compounds, conjugated alkene, amine, nitro compound, sulfonyl chloride, alkyl aryl ether and sulfoxide participated in the reduction of the metal precursor (zinc nitrate hexahydrate) into zinc oxide nanoparticles.

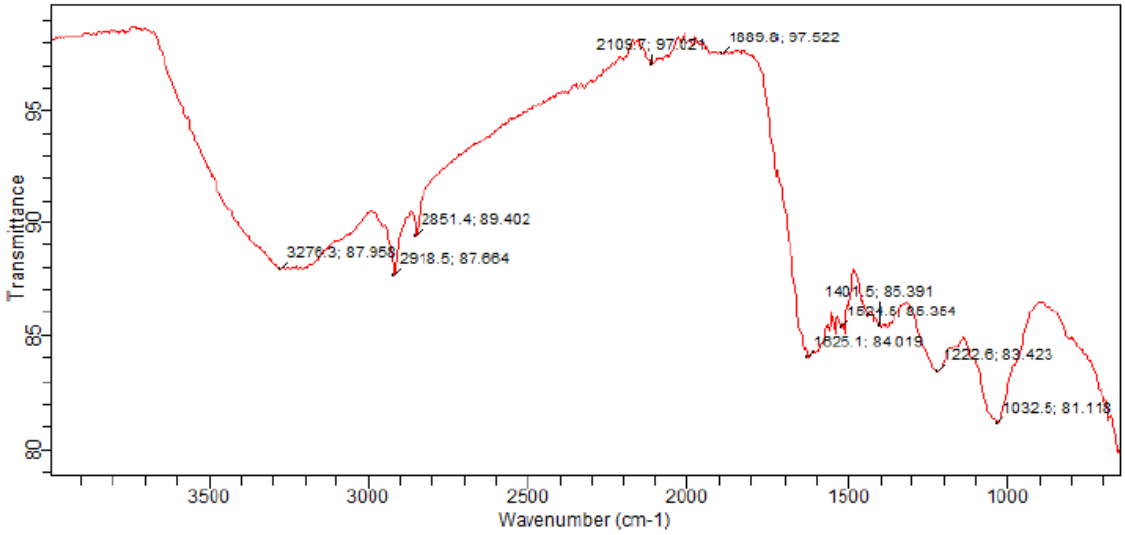

Figure 3: FTIR spectrum of ZnONPs biosynthesized with aqueous extract of *Cynodon dactylon*.

Table 2: Description of peaks in FTIR spectrum of ZnONPs

ABSORBANCE PEAK (cm^{-1})	APPEARANCE	FUCNTIONAL GROUP	COUMPOUND PRESENT
3276.3	Strong	O-H stretching	Alcohol (intermolecular bonded)
2918.5	Strong	C-H stretching	Alkyne
2851.4	Strong	N-H stretching	Amine salt
2109.7	Strong	C-H stretching	Alkane
1889.8	Weak	C≡C stretching	Alkyne
1625.1	Strong	C-H bending	Aromatic compound
		C=C stretching	Conjugated alkene
		N-H bending	Amine
1524.5	Strong	N-O stretching	Nitro compound
1401.5	Strong	S=O stretching	Sulfonyl chloride
1222.6	Strong	C-O stretching	Alkyl aryl ether
1032.5	Strong	S=O stretching	Sulfoxide

Results obtained from dynamic light scatering (DLS) analysis of the ZnONPs showed that its average size was 35.34±1.64 nm, and the polydispersity index was 0.6335. Spectrum obtained from XRD analysis of the biosynthesized ZnONPs is presented in Figure 4. The pattern revealed the crystalline structure of produced ZnO nanoparticles. There are eleven peaks on the pattern, with 2θ values of 4.62°, 9.02°, 13.46°, 31.92°, 33.28°, 34.62°, 36.44°, 47.64°, 56.84°, 63.02° and 68.16°. The peaks formed at 2θ and their corresponding orientation planes are; 31.92° (100), 34.62° (002), 36.44° (101), 47.64° (102), 56.84° (110), 63.3° (200), and 68.16° (112). The XRD pattern also revealed that crystals of ZnONPs biosynthesized using extract of *Cyodon dactylon* have hexagonal wurtzite structure. The Scherrer's formula in Equation 1, was used to estimate the size of the ZnONPs crystals;

$$L = (k\lambda/\beta \cos\theta) \quad 1$$

where L is ZnONPs crystalline size, K is Scherer's constant (K = 0.94), θ is the diffraction angle (36.42), λ is the wavelength of X-ray (1.54178 Å), and β is the full width at half maximum (FWHM) of the most intense diffraction peak that was detected to be 0.37. results showed that the estimated crystalline size was 23.6 nm, with 2θ peak positions asigned the JCPDS NO: 04-005-5076.

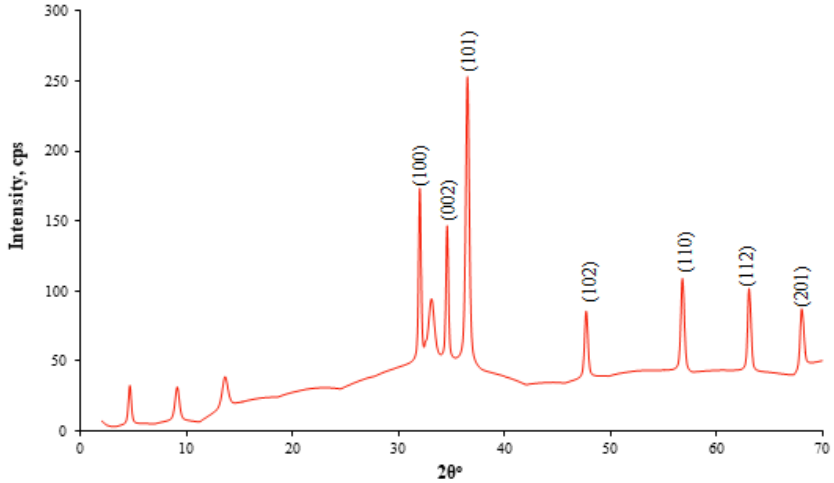

Figure 4: XRD spectrum of ZnONPs biosynthesized using *Cynodon dactylon* extract

Furthermore, Figure 5 shows the TEM micrograph of biosynthesized ZnONPs, obtained at 100 nm resolution. The micrograph indicated that the biosynthesized ZnONPs were non-uniform in sizes, ranging from 0.52 nm to 8.32 nm. The computed average was 3.96±2.4 nm. Structurally, the ZnONPs had spherical shape, no agglomeration and are poly-dispersed. The micrograph also revealed the three parts, including light, darkest, and dark, which characterize nanoparticles.

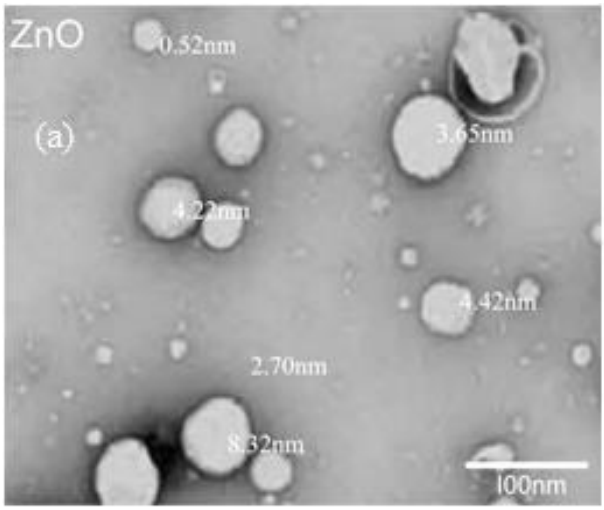

Figure 5: Transmission electron micrograph of ZnONPs biosynthesized using aqueous leaf extract of *Cynodon dactylon* at 100 nm resolutions.

Antibacterial activity of ZnONPs biosynthesized with *Cynodon dactylon* extract

Figure 6 shows the recorded inhibition zones of *Escherichia coli* and *Staphylococcus aureus* growth by different concentrations of ZnONPs, ciprofloxacin (positive control) and distilled water (negative control). Against *Staphylococcus aureus*, ZnONPs recorded 16±3.2 mm ZoI at 53.3 mg/mL concentration; 6.7±2.1 mm ZoI at 26.7 mg/mL; and 0.0±0.0 mm ZoI at 13.3 mg/mL. Ciprofloxacin and distilled water (controls) recorded 33.0±9.5 mm and 0.0±0.0 mm ZoI respectively, against *S. aureus*. On the other hand, the zones of inhibition recorded against *Escherichia coli* were 6.0±2.2 mm ZoI at 53.3 mg/mL concentration; 4.33±1.3 mm ZoI at 26.7 mg/mL; and 1.0±1.41 mm at 13.3 mg/mL. Moreover, Ciprofloxacin and distilled water produced 19.78±3.8 mm and 0.0±0.0 mm ZoI respectively, against *E. coli*. From the preceding, it is evident that *S. aureus* showed more sensitivity to all the concentrations of ZnONPs used in this study than *E. coli*. This sensitivity pattern shown by the isolates to ZnONPs was similar to the results obtained for Ciprofloxacin. However, against both *E. coli* and *S. aureus*, the inhibition zones produced by Ciprofloxacin were the highest, compared to those of ZnONPs. Analysis of the results (α = 0.05), revealed that the observed differences in ZoI between the isolates, as well as between Ciprofloxacin and 53.3 mg/mL ZnONPs on the other hand, were not significantly different.

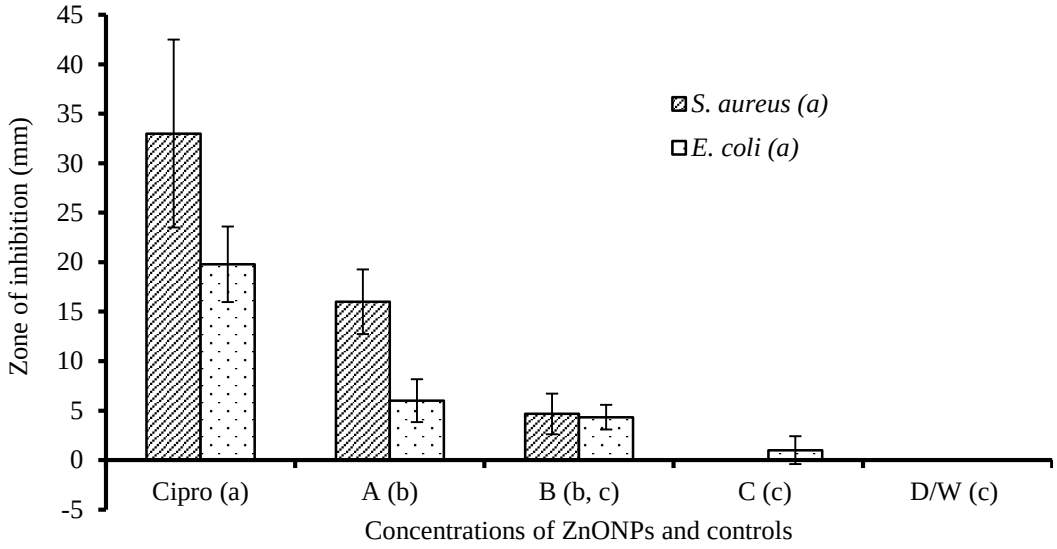

Figure 6: Sensitivities (ZoI) of bacterial isolates to biosynthesized ZnONPs at different concentrations. Samples with similar letters, in parenthesis, are not significantly different.

Antibiofilm formation activity of ZnONPs biosynthesized with *Cynodon dactylon* extract

Table 3 reveals the antibiofilm formation activities recorded by different concentrations of ZnONPs against *E. coli* and *S. aureus*. These results showed that all the concentrations of ZnONPs exhibited some activities against the bacterial isolates. Their activities were observed to be concentration-dependent, as they increased with increasing concentrations of ZnO nanoparticles. Comparatively, though activity of ZnONPs was the same against both *Staphylococcus aureus* and *E. coli*, but at the highest concentration of ZnONPs, antibiofilm formation capability of *E. coli* was more affected, than that of *Staphylococcus aureus*.

Table 3: Results of antibiofilm formation activities of biosynthesized nanoparticles

Concentrations of nanoparticles	Average antibiofilm formation activity	
	Escherichia coli	*Staphylococcus aureus*
ZnONP-A	+	++
ZnONPs-B	++	++
ZnONPs-C	+++	+++
D/W	++++	+++

where ++++ = higher biofilm; +++ = high biofilm; ++ = moderate biofilm; + = slight biofilm; A, B and C = 1.76 mg/mL, 0.88 mg/mL and 0.44 mg/mL respectively; D/W = distilled water (control).

DISCUSSION

C. dactylon extract collected from the Federal University of Technology Owerri, contains diverse groups of phytochemicals. This study has established that the phytochemicals were extractible with water, at the temperature and conditions used in this study. Some of these phytochemicals are reducing agents, which makes them essential in biosynthesis of nanoparticles.

In a previous study, phytochemical analysis of extract of *Cynodon dactylon* was reported to contain alkaloids, flavanoids, glycosides, proteins, triterpenoids steroids, terpenoides, saponins, tannins, phytosterols, resins, reducing sugars, carbohydrates, volatile oils and fixed oils (Al-Snafi, 2016). These results are similar to the result obtained in the present study. The reduction and capping of metal ions into nanoparticles have been attributed to these phytochemicals (Sabouri *et al.*, 2023). Consequently, extract of *Cynodon dactylon* would be suitable for biosynthesis of nanoparticles.

During biosynthesis, visual observation revealed that brown colour of the mixture of plant extract and precursor solution changed to dark-brown, and the solution changed to suspension/precipitate. This indicated gradual reduction and capping of the zinc nitrate hexahydrate precursor solution, into zinc oxide nanoparticles. Previous studies have reported similar colour changes (Dubey *et al.*, 2023, Çolak and Karak¨ose, 2017).

The result of absorbance of ZnONPs biosynthesized using extract of *Cynodon dactylon* showed that it can only absorb significant amount of electromagnetic waves in the UV region. This implies that the capability of the nanoparticles to become photoexcited, and generate holes, can only occur under ultraviolet light. In a previous study, report shows that when *Leonotis nepetaefolia* extract and metal ratio are reacted in 3:7 ratio, the characteristic surface plasman resonance absorption band (SPR) was in 320-370 nm region (Dubey *et al.* 2023). The absorbance peak of ZnONPs biosynthesized using extract of *Evolvulus alsinoides* was recorded at 264 nm (Yadav *et al.*, 2023). The maximum absorption peak occurred at 350 nm, with bandgap energy of 3.54 eV, showing a blue shift compared to the maximum absorption of bulk ZnO at about ~ 376 nm and bandgap energy of 3.3 eV (Gamedze *et al.*, 2023).

Accoding to Badran *et al.*, (2014), when the polydispersity index values is less than 0.3, the nanoparticles preparation is said to be monodispersed. Consequently, the ZnONPs biosynthesized in this study were polydispersed, as proven by transmission electron microscopy results. The result of this study is in line with the findings of Dubey *et al.* (2023), which indicated that using DLS, 99.9% size distribution of the ZnO nanoparticles biosynthesized with hydroethanolic extract of *Leonotis nepetaefolia* leaves, had average diameter of 9 to 18 nm, while 0.1% had average diameter of more than 20nm, without large agglomerations. Their polydispersity index was 0.6.

Similar to this study's findings, previous studies have reported functional groups of compounds in FTIR spectra. In a report, FT-IR analysis showed absorption peaks of ZnONPs from *Evolvulus alsinoides* extract as 3856, 3419, 2934, 2348, 1571, 1412, 1014, 923, 649 and 467 cm^{-1}. The weak peak detected at 3856 represented N–H stretching vibration, 3419 cm^{-1} corresponded to O–H vibration of phenolic and alcoholic compounds, long chain unsaturated fatty acids, octadecanoic acids, squalene (triterpine, a phenolic compounds), piperine, n-hexdecanoic acid and cholesterol (Yadav *et al.*, 2023). Furthermore, the spectrum of ZnONPs from hydroethanolic extract of *Leonotis nepetaefolia* leaves, showed peaks characteristic of the OH elongations at 3283 cm^{-1} belonging to hydroxyl groups. Bands representing –CH< occurred at 2933 cm^{-1}; for >C=O it occurred at 1604 cm^{-1}; for carbonyl group stretching, it occurred at 1396 cm^{-1}. Other bands representing the stretching and bending of C-O bonds were detected between 1000 and 1100 cm^{-1}. Bands corresponding to alkenes of terpenes, monoterpenes and sesquiterpenes were observed at 1604 cm^{-1} (Dubey *et al.*, 2023).

In comparison to the X-ray diffraction (XRD) spectrum recorded in this study, the XRD patterns of ZnONPs biosynthesized using *Mucuna pruriens* extract revealed eight diffraction peaks, corresponding to 100, 002, 101, 102, 110, 103, 200 and 112 lattice planes, with JCPDS Card No: 00-036-1451, which confirmed the successful biosynthesis of ZnONPs. The size of ZnONPs crystallite obtained using Scherrer's equation was 46.5 nm (Gamedze *et al.*, 2023). Similarly, Yadav *et al.* (2023) had reported that the peaks observed in XRD pattern of ZnONPs from extract of *Evolvulus alsinoides* were at 2θ 31.84°, 34.52°, 36.33°, 47.63, 56.71°, 62.96, 68.13° and 69.18°, which corresponded to refraction plane 100, 002, 101, 110, 103, 112. As suggested by Dubey *et al.* (2023), other peaks observed on the XRD pattern of ZnONPs biosynthesized in this study could be attributed to components of the extract, which participated in reductive formation of the nanoparticles.

The ZnONPs biosynthesized in the present study were smaller than those reported by Gamedze *et al.* (2023), which though were spherical as well, but their particle sizes ranged from 21.60 to 47.16 nm, with an average of 30.50 nm. Dubey *et al.* (2023) reported that ZnONPs showed irregular shapes, with distinguishable semi-circles (ovoid) and size distribution in the 20 to 40 nm range.

Antibacterial activities of biosynthesized ZnO nanoparticles

Corresponding to the results of antibacterial analysis of this study, Thi *et al.* (2020) had reported that at 0.025 mg mL^{-1}, ZnONPs biosynthesized using orange fruit peel extract demonstrated strong antibacterial activity against isolates of *Staphylococcus aureus* and *Escherichia coli*, after 8 hours of incubation in the absence of UV illumination. The zones of inhibition of bacterial growth recorded in the present study were higher that the results reported in a similar previous study, in which biosynthesized ZnONPs recorded zones of inhibition of 10 ± 0.624 mm against *Staphylococcus aureus*, and 10 ± 0.493 mm against *E. coli* (Chauhan *et al.*, 2020). Similarly, as observed in the present study, ampicillin used as positive control had higher zone of inhibition than ZnONPs.

Antibiofilm formation activity of biosynthesized ZnO nanoparticles

This study showed that ZnONPs produced some antibiofilm formation activity against *E. coli* and *S. aureus*, with higher activity recorded

against *E. coli*. This finding has been corroborated in another report which indicated that the ZnONPs demonstrated 82.42% and 84.69% antibiofilm formation activity against *S. aureus* and *P. aeruginosa* respectively, at concentration of 512 mg/mL (Kang *et al.*, 2022). Also, green-synthesized ZnONPs was reported to produce 95.27±1.28% and 92.27±1.22% antibiofilm formation activity against *A. faecalis* and *P. gingivalis* respectively (Lahiri *et al.*, 2022).

CONCLUSION

Result obtained from the study demonstrated that aqueous extract of *Cynodon dactylon* Pers. is composed of phytochemical which makes it suitable for reduction and capping of metal ions to form nanoparticles. Characterization of biosynthesized ZnONPs met known characteristics identifiable using UV visible spectrophotometer, Fourier transform infrared spectroscopy, dynamic light scattering, X-ray diffraction and transmission electron microscopy. It produced dose-dependent effective against E. coli and S. aureus clinical isolates by subjecting it to antibacterial and antibiofilm formation analyses. Therefore, *Cynodon dactylon* extract can be exploited in the field of nanotechnology.

REFERENCES

Akujobi, C. O., Anuforo, H. U., Okereke, J. N., Ibeh, C. and Agbo, C. J. (2020). Parametric optimization of synthesis of silver nanoparticles from *Mangifera indica* and *Prunus dulcis* extracts and their antibacterial activity. *Analele Universității din Oradea, Fascicula Biologie,* 27(1): 21-26.

Al-Shabib, N., Husain, F., Hassan, I., Khan, M., Ahmed, F., Qais,Faizan, M., Oves, R. M., Khan, R. A., Khan, M., Ahmad, I. and Al-Tamimi, J. (2018). Biofabrication of zinc oxide nanoparticle from *Ochradenus baccate* leaves: Broad-spectrum antibiofilm activity, protein binding studies, and in vivo toxicity and stress studies. *Journal of Nanomaterials,* 8612158: 1-15. **[Crossref]**

Al-Snafi, A. E. (2016). Chemical constituents and pharmacological effects of *Cynodon dactylon*: A review. *IOSR Journal of Pharmacy,* 6(7): 17-31. **[Crossref]**

Amini, N., Amin, G. and Jafari, A. Z. (2017). Green Synthesis of Silver Nanoparticles using *Avena sativa* L. Extract. *Nanomedicine Research Journal,* 2(1): 57-63. **[Crossref]**

Angham, T. A. and Lekaa, K. A. K. (2023). Biosynthesis, characterization, adsorption and antimicrobial studies of vanadium oxide nanoparticles using *Punica granatum* extract. *Baghdad Science Journal,* 2023: 1-12.

Aritonang, H. F., Koleangan, H. and Wuntu, A. D. (2019). Synthesis of Silver Nanoparticles using Aqueous Extract of Medicinal Plants (*Impatiens balsamina* and *Lantana camara*) Fresh Leaves and Analysis of Antimicrobial Activity. *International Journal of Microbiology,* 1: 1-8. **[Crossref]**

Badran, M. (2014). Formulation and *In Vitro* Evaluation of Flufenamic Acid Loaded Deformable Liposomes for Improved Skin Delivery. *Digest Journal of Nanomaterials and Biostructures,* 9: 1-12.

Banu, K. S. and Catherine, L. (2015). General Techniques Involved in Phytochemical Analysis. *International Journal of Advanced Research in Chemical Science,* 2(4): 25-32.

Bukhari, A., Ijaz, I., Gilani, E., Nazir, A., Zain, H., Saeed, R., Alarfaji, S. S., Husain, S., Aftab, R. and Naseer, Y. (2021). Green using different plants' parts for antimicrobial and anticancer activity. *Coatings,* 11(11): 1374. 1-17. **[Crossref]**

Chauhan, A., Verma, R., Kumari, S., Sharma, A., Shandilya, P., Li, X., Batoo, K. M., Imran, A., Kulshrestha, S. and Kumar, R. (2020). Photocatalytic dye degradation and antimicrobial activities of pure and Ag-doped ZnO using *Cannabis sativa* leaf extract. *Scientific Reports,* 10(7881): 1-16. **[Crossref]**

Çolak, H. and Karak¨ose, E. (2017). Green synthesis and characterization of nanostructured ZnO thin films using *Citrus aurantifolia* (lemon) peel extract by spin-coating method. *J. Alloys Compd.,* 690: 658–662. **[Crossref]**

Dubey, A., Dwivedi, M., Shukla, B. P., Kumar, A. and Tripathi, A. K. (2023). Phytochemistry and biological uses of *Leonotis nepetaefolia* (L.) R.BR. ethanolic extract zinc oxide nanoparticles. *Journal of Complementary Medicine Research,* 14(5): 85-97. **[Crossref]**

Ejikeme, C. M., Ezeonu, C. S. and Eboatu, A. N. (2014). Determination of Physical and Phytochemical Constituents of Some Tropical Timbers Indigenous to Niger Delta Area of Nigeria. *European Scientific Journal*, 10(18): 247-270.

El-Hawary, S., Almaksoud, H., Saber, F., Elimam, H., Sayed, A., El-Raey, M. and Abdelmohsen, U. (2021). Green-synthesized zinc oxide nanoparticles, anti-Alzheimer potential and the metabolic profiling of Sabalblack burniana grown in Egypt supported by molecular modelling. *RSC Advances,* 11: 18009–18025. **[Crossref]**

Erdogan, O., Abbak, M., Demirbolat, G. M., Birtekocak, F., Aksel, M. Pasa, S. and Cevik, O. (2019). Green Synthesis of Silver Nanoparticles Via *Cynara scolymus* Leaf Extracts: The Characterization, Anticancer Potential with Photodynamic Therapy in

MCF7 Cells. *PLoS ONE*, 14(6): 1-15. **[Crossref]**

Gamedze, N. P., Mthiyane, M. N., Mavengahama, S., Singh, M. and Onwudiwe, D. C. (2023). Biosynthesis of ZnO nanoparticles using the aqueous extract of *Mucuna pruriens* (utilis): Structural characterization, and the anticancer and antioxidant activities. *Chemistry Africa*, 2023: 1-10. **[Crossref]**

Gungure, A., Jule, L., Ramaswamy, S., Priyanka, D. L., Gudata, L., Nagaraj, N., Mekonen, A. B., and Ramaswamy, K. (2021). Green synthesis and characterizations of zinc oxide (ZnO) nanoparticles using aqueous leaf extracts of coffee (*Coffea arabica*) and its application in environmental toxicity reduction. *Journal of Nanomaterials*, 2: 1-6. **[Crossref]**

Husain, F. M., Qais, F. A., Ahmad, I., Hakeem, M. J., Baig, M. H. and Masood K. J. (2022). Biosynthesized zinc oxide nanoparticles disrupt established biofilms of pathogenic bacteria. *Applied Sciences*, 12(710): 1-15. **[Crossref]**

Kang, M. G., Khan, F., Jo, D. M., Oh, D., Tabassum, N. and Kim, Y. M. (2022). Antibiofilm and antivirulence activities of gold and zinc oxide nanoparticles synthesized from Kimchi-Isolated *Leuconostoc sp.* strain C2. *Antibiotics*, 11(1524): 1-23. **[Crossref]**

Kulkarni, S. B., Patil, U. M., Salunkhe, R. R., Joshi, S. S. and Lokhande, C. D. (2011). Temperature impact on morphological evolution of ZnO and its consequent effect on physicochemical properties. *Journal of Alloys Compounds*, 509(8): 3486-3492. **[Crossref]**

Kumavat, S. R. and Mishra, S. (2021). Green synthesis of silver nanoparticles using *Borago officinalis* leaves extract and screening its antimicrobial and antifungal activity. *International Nano Letters*, 1-15. **[Crossref]**

Lahiri, D., Ray, R. R., Sarkar, T., Upadhye, V. J., Ghosh, S., Pandit, S., Pati, S., Edinur, H. A., Abdul, K. Z., Nag, M. and Ahmad, M. M. R, (2022) Anti-biofilm efficacy of green-synthesized ZnO nanoparticles on oral biofilm: *In vitro* and *silico* study. *Frontiers in Microbiology* 13(939390): 1-17. **[Crossref]**

Mahamadi, C. and Wunganayi, T. (2018). Green Synthesis of Silver Nanoparticles using *Zanthoxylum chalybeum* and their Antiprolytic and Antibiotic Properties. *Cogent Chemistry*, 4: 1-12. **[Crossref]**

Raaman, N. (2006). Phytochemical Techniques. New India Publishing Agency, New Delhi, pp.19-25. **[Crossref]**

Sabouri, Z., Kazemi-Oskuee, R., Sabouri, S., Tabrizi, H. M. S. S., Samarghandian, S., Sajid-Abdulabbas, H. and Darroudi, M. (2023). Phytoextract-mediated Synthesis of Ag-doped ZnO-MgO-CaO Nanocomposite using *Ocimum basilicum* L Seeds Extract as a Highly Efficient Photocatalyst and Evaluation of their Biological Effects. *Ceramic International*, 49(12): 20989-20997. **[Crossref]**

Saxena, M., Saxena, J., Nema, R., Singh, D. and Gupta, A. (2013). Phytochemistry of Medicinal Plants. *Journal of Pharmacognosy and Phytochemistry*, 1(6): 168-182.

Sigma-Aldrich (2023). Infrared Spectrum Table and Chart. Retrieved from www.sigmaaldrich.com on 19th September, 2023.

Smaoui, S., Chérif, I., Ben-Hlima, H., Khan, M., Rebezov, M., Thiruvengadam, M., Sarkar, T., Shariati, M. A. and Lorenzo, J. M. (2023). Zinc oxide nanoparticles in meat packaging: A systematic review of recent literature. *Food Packaging and Shelf Life*, 36(101045): 1-20. **[Crossref]**

Taylor, P. (2013). Synthesis, antibacterial activity, antibacterial mechanism and food applications of ZnO nanoparticles: a review. *Food Additive and Contamination*, Part A, 31(2): 1-14. **[Crossref]**

Thakur, A., Thakur, P. and Khurana, S. M. P. (2022). Synthesis and applications of nanoparticles. *Springer Nature*, 459: 1-17. **[Crossref]**

Thi, T. U. D., Nguyen, T. T., Thi, Y. D., Thi, K. H. T., Phan, B. T., and Pham, K. N. (2020). Green synthesis of ZnO nanoparticles using orange fruit peel extract for antibacterial activities. *Royal Society of Chemistry Advances*, 10: 23899-23907. **[Crossref]**

Turan, N. B., Erkan, H. S., Engin, G. O. and Bilgili, M. S. (2019). Nanoparticles in the aquatic environment: Usage, properties, transformation, and toxicity. *Process for Safe Environment*, 1(130): 238-49. **[Crossref]**

Yadav, A., Jangid, N. K. and Khan, A. U. (2023). Biogenic synthesis of ZnO nanoparticles from *Evolvulus alsinoides* plant extract. *Journal of Umm Al-Qura University for Applied Sciences*, 2023: 1-7. **[Crossref]**

Zhao, J., Yan, P., Qureshi, A. and Chiang, Y. W. (2023). How do material characteristics and antimicrobial mechanisms affect ? *Blue-Green Systems*, 00(0): 1-27.